

Sheared dipolar suspensions

J. R. Melrose

Department of Chemistry, University of Surrey, Guildford, Surrey GU2 5XH, United Kingdom

(Received 22 July 1991)

Simulated sheared suspensions of particles with dipole interactions are found to adopt a number of different structural and rheological phases including a novel *flowing crystalline* phase. A crossover from Brownian to Stokesian transitions between phases is driven by particle-size effects.

PACS number(s): 47.50.+d, 62.15.+i, 82.70.Dd, 81.30.-t

Experimental [1-5] and simulation [6-8] studies of suspensions of interacting particles reveal a variety of phases which possess ordered structures under shear. Structure underlies [1,5-8] non-Newtonian rheology. Suspensions of polarizable particles form columnar aggregates [9,10] under an applied field and these cause [11] the suspension to develop a dynamic yield stress and a viscosity enhancement known as the electrorheological (ER) effect [10-12]. The present work examines, by simulation, structure in the bulk of a model suspension of polarizable particles under shear. Current thinking suggests that [10,13,14] polarization and hydrodynamic interactions determine the ER effect; here, Brownian forces are included.

A complete treatment of sheared suspensions would include many-body hydrodynamics. Elegant techniques for approximating these have been developed [15]—to date, however, these $O(N^3)$ methods have only been able to simulate the dynamics of small monolayer systems. Under simple shear all three spatial directions are distinct and it is necessary to predict the structure of sheared strongly interacting systems in full three-dimensional (3D) space. To make progress, the present work follows a number of authors [6,7,16-18] and considers an $O(N^2)$ algorithm [6] which neglects many-body hydrodynamics. While quantitative accuracy of viscosities must therefore be abandoned, intriguingly these algorithms do show the non-Newtonian rheologies of experiment [6]. The working hypothesis is that these algorithms also give qualitatively correct predictions for structure under shear.

The simulation model [16-19] consists of particles interacting via repulsive and point-dipole interactions suspended in a fluid medium represented by Brownian forces and a viscous drag. Simple shear at a rate $\dot{\gamma}$ is applied to a bulk periodic system by use of periodic sliding boundary conditions [6].

The simulation algorithm [6] is a linearized version of the position Langevin equation describing overdamped motion in a viscous medium. The q th coordinate of the i th particles position is updated over a time step h by

$$r_{iq}(t+h) = r_{iq}(t) + [F_{iq}(t) + R(t,h)]h/m\xi + \dot{\gamma}r_{vi}(t)h\delta_{qv}, \quad (1)$$

where the friction coefficient $\xi = 3\pi\eta_s\sigma/m$, η_s is the viscosity of the fluid, σ and m are the particle diameter and mass. Following Ref. [2], \mathbf{V} denotes the direction of

shear velocity, ∇ the direction of shear gradient, and \mathbf{e} the third direction (see Fig. 1). The final term in (1) imposes the shear gradient along ∇ ; F and R denote the particle interactions and fluid random Brownian forces, respectively. This level of algorithm corresponds to the free-draining approximation of polymer dynamics. The interparticle forces are derived from the potential

$$\phi = \sum_{i,j} akT/(\sigma/r_{ij})^n + \sum_{i,j} Q(kT)(1 - 3r_{ij}^2/r_{ij}^2)/(r_{ij}/\sigma)^3, \quad (2)$$

where the dimensionless interaction strength Q is related to the particle dipole moment $\mu(E)$:

$$Q = (4\pi kT\epsilon_0\epsilon_s\sigma^3)^{-1}\mu^2. \quad (3)$$

ϵ_s is the dielectric constant of the fluid. Real particles in an ER suspension will have complex core interactions due to lubrication, rough surface, and most likely polymer coating (added to provide steric stabilization). In the spirit of this simplified study the model includes a steep power-law core repulsion with exponent n and dimensionless interaction strength α ; set here to unity. The core does introduce some ambiguity in the definition of particle diameter and volume fraction. The dipoles $\mu(E)$ are fixed in alignment parallel to a uniform field E along ∇ (see Fig. 1). The aligned dipole interactions are truncated cubically [20]. A real ER suspension will have stronger many-body multipolar and hydrodynamic interactions. A simulation of a small monolayer system using $O(N^3)$ techniques for these, but without Brownian forces, has been reported [21], but suffers from the reduced dimensionality argued above to be inappropriate. The neglect of particle

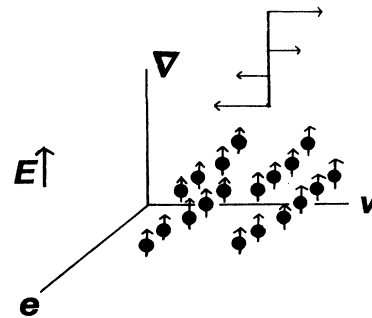


FIG. 1. The computational geometry.

rotation assumes that the particles are freely rotating in the shear flow. Particle rotation will couple with the relaxation of its polarization [12]. Here this relaxation is assumed to be so fast that this coupling can be neglected.

The shear rate represented as a dimensionless Péclet number setting the relative magnitude of the shear to Brownian forces: $Pe = \dot{\gamma}\tau_r$, where τ_r is the time that one isolated particle coordinate would take to diffuse its radius:

$$Pe = 3\pi\eta_s\sigma^3\dot{\gamma}/8kT. \quad (4)$$

If it is assumed that [13] $\mu(E) \propto \sigma^3$, the model has just four parameters: Pe , Q , the repulsion exponent (n), and the volume fraction ϕ_V defined on σ . Systems of the same ϕ_V are equivalent in that they map onto the same Q and Pe . The particle diameter σ is implicit in the model: for a given $\dot{\gamma}$ and E , systems of decreasing σ map via Eqs. (3) and (4) onto decreasing values of Pe and Q .

The present study fixes ϕ_V to 0.3 and n to 36. A system of $N=108$ particles was simulated at points along many trajectories in the space (Q, Pe) ; those discussed below are shown in Fig. 2. A longer report will be published [22]. Several quantities were monitored, including the relative apparent viscosity η_r

$$\eta_r = 1 + \frac{5}{2}\phi_V + \eta_p, \quad (5)$$

where η_p is the contribution to the viscosity due to the stress, $\langle\tau_p\rangle$, of the particle interactions averaged over a simulation run: $\eta_p = -\langle\tau_p\rangle/(\eta_s\dot{\gamma})$ and η_s is the solvent viscosity. The Einstein contribution is implicit in the viscous drag included in the algorithm. Structure was probed by use of

$$S_{qM} = N^{-2} \left| \sum_j \exp[iM(2\pi/s)r_{jq}] \right|^2, \quad (6)$$

where s is the computational box-side length. Transitions involving M layers forming normal to the dimension q ($q = \mathbf{V}, \mathbf{V}$, or \mathbf{e}) are signaled by sudden increases in S_{qM} .

As illustrated in Fig. 2, three distinct phases exist in the space (Q, Pe) : a liquid phase (L), a flowing crystalline phase (FC), and a hexagonal shear string phase (HSS)

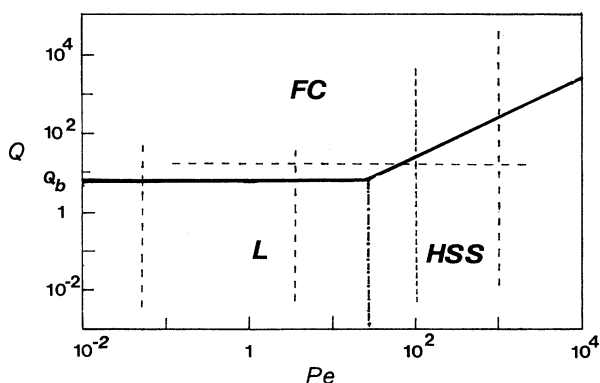


FIG. 2. Phase diagram L : liquid phase; HSS : shear string phase; FC : flowing crystalline phase. Solid lines show phase transitions, dashed lines indicate some of the trajectories along which simulations were made. Dash-dotted curve indicates a weak liquid to shear string phase boundary.

[6,8,23]. Figure 3 shows various configurations. Transitions between these phases result from the competition between the Brownian, dipole, and shear viscous forces. In the absence of shear, $Pe=0$, for $Q >$ (some) Q_b the dipole forces dominate the Brownian forces and the particles alter from an amorphous structure, $Q < Q_b$, into a gel

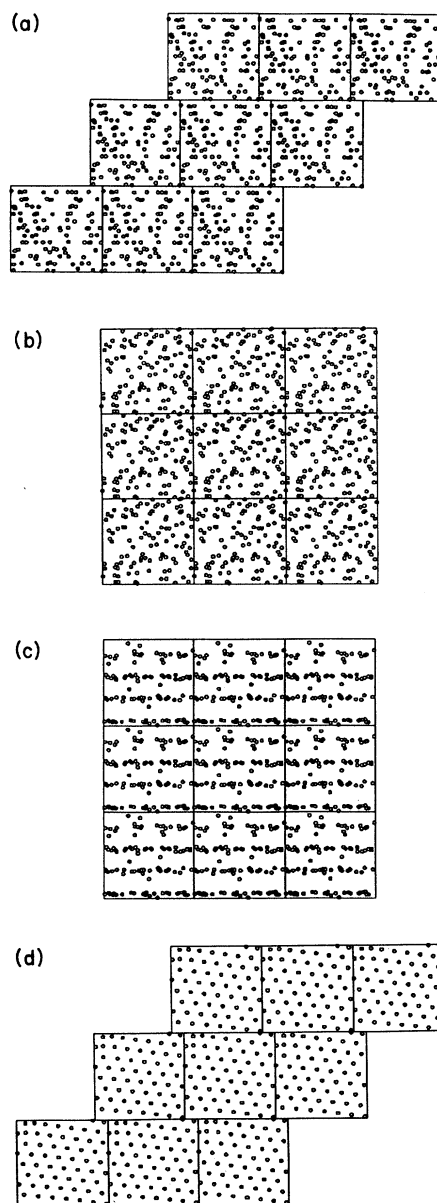


FIG. 3. Several projected configurations along $Pe=1000$. The dots indicate the particle centers (to gauge their full size, note that the box-side length is 5.646σ). The computational box is shown with its nearest-neighbor periodic images. (a) A projection onto (\mathbf{V}, \mathbf{V}) in the shear string phase at $Mn=10$; note the strings in the \mathbf{V} direction. (b) A projection onto (\mathbf{e}, \mathbf{V}) at $Mn=1$; note no (\mathbf{V}, \mathbf{V}) layers are evident. (c) A projection onto (\mathbf{e}, \mathbf{V}) at $Mn=10^{-0.75}$; note four (\mathbf{V}, \mathbf{V}) layers have appeared. (d) A projection onto (\mathbf{V}, \mathbf{V}) of one of two layers present at $Mn=10^{-2.4}$; note its strained hexagonal order.

$Q > Q_b$ orientated along E [10,16,17]; this is the equilibrium phase transition. In the present model, $n=36$, $N=108$, and $\phi_V=0.3$, I find $6.5 < Q_b < 7$. At low Pe and Q a liquid phase with no discernible long-range order exists. At higher Pe ($Pe > 20$) and low enough Q , in the hexagonal shear string phase, the particle interactions are dominated by the shear and repulsive core; they form strings along \mathbf{V} which in the present case are ordered in a 6×6 hexagonal pattern in the (\mathbf{V}, \mathbf{e}) plane. In the present case for low enough Q and between $Pe=20$ and 50 S_{V6} and S_{V6} increase by a factor of 3–4 over the liquid phase values (ca. 10^{-2} for all q and M). Throughout the L phase the system shear thins with the viscosity dropping (independent of Q) as [6] $Pe^{-\beta}$ with $\beta=0.08 \pm 0.01$. In the HSS phase $\eta_r = 1 + \frac{5}{2} \phi_V + \delta(Q, Pe)$ where the particle contribution $\delta(Q, Pe) \ll 1$. The competition between the viscous and dipole forces is set by the Mason number Mn [13]. In terms of (3) and (4) [17],

$$Mn = Pe/12Q. \quad (7)$$

For a given $Pe > 20$ as Q is increased the HSS phase persists and then degrades just below Mn_c . At Mn_c the particles reorder into a FC phase; the S_{qM} signature of the HSS phase is lost and in the present model for $Mn = 10^{-0.4} < Mn_c < 10^{-0.6}$ it is replaced with an abrupt tenfold increase in S_{e4} : four layers form in (\mathbf{V}, \mathbf{V}) planes normal to \mathbf{e} (see Fig. 3). The individual layers are 2D lattices with defects which flow by both defect propagation and periodically straining to a maximum at which they relax and reorder [22]. Further increases in Q can cause the layers to aggregate under the dipole interactions and form paired or tripled layers. The competition at Mn_c between shear and interaction forces is classified here as a *Stokesian transition*. On decreasing Q the layers persist below Mn_c .

When $Q_c = Pe/12Mn_c < Q_b$ the dipole and shear competition crosses over to a dipole and Brownian competition. The model displays [16,21] an effective critical Mason number Mn_c (eff) $\cong Pe/12Q_b$ at which the layering transition from the L to the FC phase occurs; this competition between Brownian (thermal) and interaction forces is here defined as a *Brownian transition*. It is the extension of the equilibrium transition of the system. The term Brownian transition is introduced deliberately here. The crossover from Stokesian to Brownian transitions can be driven by decreasing particle size; a feature highly relevant to ER fluid design. Simulations [22] at several $Pe < 20$ indicate a horizontal boundary from $Q = Q_b$ to $Pe = 12Q_b Mn_c$.

Plots of η_r vs Mn data for runs at fixed Pe and varying Q are shown in Fig. 4. At high Mn they all show the HSS or L phase plateaus in viscosity (the former close to constant, the latter varying as $Pe^{-\beta}$) and in the FC phase, starting at some $Mn < Mn_c$, an enhanced viscosity with $\eta_r \propto Mn^{-\alpha}$. A significant increase in viscosity occurs only some way past Mn_c ; quite generally, noticeable changes in rheology are not in exact coincidence with structural changes, the shear thinning through the L phase is all but completed before the HSS structure emerges. The runs at

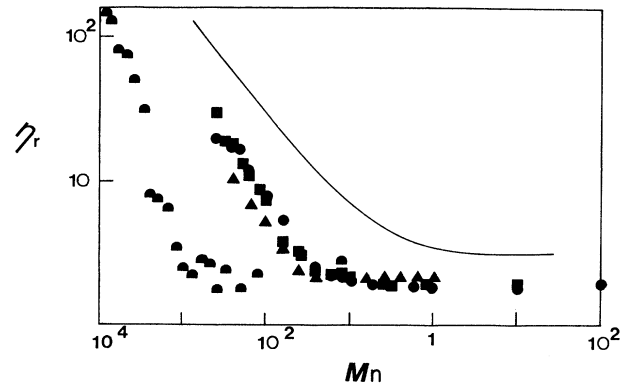


FIG. 4. η_r vs Mn data for the runs at $Pe=10^2$ (■), $Pe=10^3$ (●); $Pe=5$ (▲), and $Pe=0.05$ (◆). The solid curve sketches the path of the same plot of the experimental data of Ref. [13] at $\phi_V=0.23$.

$Pe=10^2$ and 10^3 collapse onto the same plot, with the exponent $\alpha=0.96 \pm 0.04$. This universal plot and data collapse for the model is qualitatively the same as that recently reported for ER suspensions [13,14].

The runs at $Pe=0.05$ and 5 do not show universality; they rise off their plateaus in viscosity at lower Mn , varying with Pe according to the line of Brownian transitions. In the FC phase above the Brownian line, the viscosity exponent $\alpha > 1$ and it varies with Pe (along $Pe=0.05$, $\alpha=1.8 \pm 0.2$). The extent upwards in Q of this breakdown in universality was not studied. Data for η_r of a trajectory at $Q=16$ (see Fig. 2) follows the universal plot until low Pe where it deviates to lower values.

The soft core leads to some ambiguity in the particle size: at high Pe and Q the particles push in against the core. The effect is not significant across the Brownian regime but at $Pe=10^2$ and 10^3 the particles—across the Stokesian transition—have an effective diameter determined from the first peak of the radial distribution function of 0.96σ and 0.91σ , respectively. While the detailed structure within a layer is influenced by the softness of the core, the fundamental layering transition is not.

The results here predict that ER suspensions will adopt a layered crystalline phase, in contrast to the previously proposed chain model [11]. The model extends previous ER studies [13,14,21] by including particle-size effects. As σ is decreased for fixed ϕ_V , a given operating range of $\dot{\gamma}$ and E will map onto decreasing Q and Pe . If σ is too small, then the crossover from Stokesian to Brownian transitions will require higher fields to achieve the enhanced viscosity. The model provides one of the first predictions of a nonequilibrium phase diagram for strongly interacting sheared suspensions.

I thank Castrol Research for financial support and D. Heyes, H. Block, L. Woodcock, and N. Webb for useful conversations.

- [1] R. L. Hoffman, *J. Colloid Interface Sci.* **46**, 491 (1974).
- [2] B. J. Ackerson and N. A. Clark, *Phys. Rev. Lett.* **46**, 123 (1981); *Phys. Rev. A* **30**, 906 (1984); *Physica* **118A**, 221 (1983).
- [3] B. J. Ackerson, J. B. Hayter, N. A. Clark, and L. Cotter, *J. Chem. Phys.* **84**, 2344 (1986).
- [4] M. Tomita and T. G. M. Van De Ven, *J. Colloid Interface Sci.* **99**, 374 (1984).
- [5] L. B. Chen and C. F. Zukoski, *Phys. Rev. Lett.* **65**, 44 (1990).
- [6] D. M. Heyes, *Comput. Phys. Rep.* **8**, 73 (1988); *Phys. Lett. A* **132**, 399 (1988); *J. Non-Newtonian Fluid Mech.* **27**, 47 (1988).
- [7] W. Xue and G. S. Grest, *Phys. Rev. Lett.* **64**, 1409 (1990).
- [8] J. L. Erpenbeck, *Phys. Rev. Lett.* **52**, 1333 (1984); L. V. Woodcock, *Phys. Rev. Lett.* **54**, 1513 (1985).
- [9] S. Fraden, A. J. Hurd, and R. B. Meyer, *Phys. Rev. Lett.* **63**, 2373 (1989).
- [10] A. P. Gast and C. F. Zukoski, *Adv. Colloid Interface Sci.* **30**, 153 (1989).
- [11] W. M. Winslow, *J. Appl. Phys.* **20**, 1137 (1949).
- [12] H. Block and J. P. Kelly, *J. Phys. D* **21**, 1661 (1988).
- [13] L. Marshall, C. F. Zukoski IV, and J. W. Goodwin, *J. Chem. Soc. Faraday Trans. 1* **85**, 2785 (1989).
- [14] D. J. Klingenberg, D. Dierking, and C. F. Zukoski, *J. Chem. Soc. Faraday Trans. 1* **87**, 425 (1991).
- [15] L. Durlofsky, J. F. Brady, and G. Bossis, *J. Fluid Mech.* **180**, 21 (1987).
- [16] P. Bailey, D. G. Gillies, D. M. Heyes, and L. H. Sutcliffe, *Mol. Sim.* **4**, 137 (1989).
- [17] D. M. Heyes and J. R. Melrose, *Mol. Sim.* **5**, 293 (1990).
- [18] D. J. Klingenberg, F. van Swol, and C. F. Zukoski, *J. Chem. Phys.* **91**, 7888 (1989).
- [19] M. Whittle, *J. Non-Newtonian Fluid Mech.* **37**, 223 (1991).
- [20] The use of Ewald sums in sliding periodic boundary conditions is nontrivial and long-range corrections to dipolar forces in simulations are known to be marginal for first-order ensemble averages. Moreover, with aligned dipoles the coupling of orientational fluctuations over long range—the usual motivation for including long-range corrections—is absent. Simulations with both $N=108$ and 256 particles with both cubic and spherical truncations show no significant variation.
- [21] R. T. Bonnecaza and J. F. Brady, in *Proceedings of the II International Conference on Electrorheological Fluids*, edited by H. Conrad, A. F. Spercher, and J. D. Carlson (Technomic, Lancaster, 1990).
- [22] J. R. Melrose (unpublished).
- [23] A. J. Hopkins, F. S. Jardali, and L. V. Woodcock, *Mol. Sim.* **4**, 241 (1989).